Article

Cell Reports

Macaques Exhibit Implicit Gaze Bias Anticipating Others' False-Belief-Driven Actions via Medial Prefrontal Cortex

Graphical Abstract

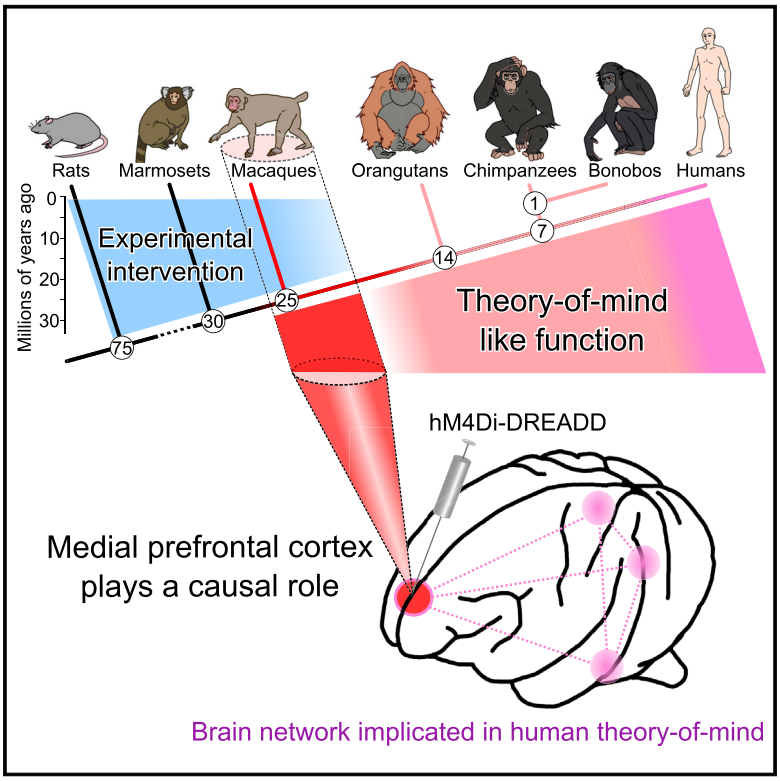

Highlights

- Macaques exhibit implicit gaze bias anticipating others' false-belief-driven actions
- Inhibitory DREADDs silencing medial prefrontal neurons abolish the gaze bias
- Macaques and humans share brain networks for false-belief attribution-like behaviors
- Among the network, the medial prefrontal cortex is causally linked to mental attribution

Authors

Taketsugu Hayashi, Ryota Akikawa, Keisuke Kawasaki, ..., Atsuhiko Iijima, Toshiyuki Someya, Isao Hasegawa

Correspondence

psy@med.niigata-u.ac.jp (T.S.), ihasegawa-nsu@umin.ac.jp (I.H.)

In Brief

Hayashi et al. ask whether only hominids possess theory of mind. They show macaques' implicit gaze bias anticipating others' false-belief-guided actions, which is abolished by chemogenetic silencing of the medial prefrontal cortex. Thus, false-belief attribution-like behaviors of non-human primates are underpinned by shared neuronal mechanisms with humans.

Hayashi et al., 2020, Cell Reports *30*, 4433–4444
March 31, 2020
https://doi.org/10.1016/j.celrep.2020.03.013

CellPress

Cell Reports
Article

Macaques Exhibit Implicit Gaze Bias Anticipating Others' False-Belief-Driven Actions via Medial Prefrontal Cortex

Taketsugu Hayashi,[1,2,8] Ryota Akikawa,[2,3,8] Keisuke Kawasaki,[2] Jun Egawa,[1] Takafumi Minamimoto,[4] Kazuto Kobayashi,[5] Shigeki Kato,[5] Yukiko Hori,[4] Yuji Nagai,[4] Atsuhiko Iijima,[3,6,7] Toshiyuki Someya,[1,*] and Isao Hasegawa[2,9,*]

[1]Department of Psychiatry, Niigata University Graduate School of Medical and Dental Sciences, Niigata, Japan
[2]Department of Physiology, Niigata University School of Medicine, Niigata, Japan
[3]Graduate School of Science and Technology, Niigata University, Niigata, Japan
[4]Functional Brain Imaging, National Institute of Radiological Sciences, National Institute for Quantum and Radiological Science and Technology, Chiba, Japan
[5]Department of Molecular Genetics, Institute of Biomedical Sciences, Fukushima Medical University, Fukushima, Japan
[6]School of Health Sciences, Faculty of Medicine, Niigata University, Niigata, Japan
[7]Interdisciplinary Program of Biomedical Engineering, Assistive Technology, and Art and Sports Sciences, Faculty of Engineering, Niigata University. Niigata, Japan
[8]These authors contributed equally
[9]Lead Contact
*Correspondence: psy@med.niigata-u.ac.jp (T.S.), ihasegawa-nsu@umin.ac.jp (I.H.)
https://doi.org/10.1016/j.celrep.2020.03.013

SUMMARY

The ability to infer others' mental states is essential to social interactions. This ability, critically evaluated by testing whether one attributes false beliefs (FBs) to others, has been considered to be uniquely hominid and to accompany the activation of a distributed brain network. We challenge the taxon specificity of this ability and identify the causal brain locus by introducing an anticipatory-looking FB paradigm combined with chemogenetic neuronal manipulation in macaque monkeys. We find spontaneous gaze bias of macaques implicitly anticipating others' FB-driven actions. Silencing of the medial prefrontal neuronal activity with inhibitory designer receptor exclusively activated by designer drugs (DREADDs) specifically eliminates the implicit gaze bias while leaving the animals' visually guided and memory-guided tracking abilities intact. Thus, neuronal activity in the medial prefrontal cortex could have a causal role in FB-attribution-like behaviors in the primate lineage, emphasizing the importance of probing the neuronal mechanisms underlying theory of mind with relevant macaque animal models.

INTRODUCTION

In social interactions among individuals, the ability to understand unobservable mental states of others, such as beliefs, intentions, or desires, is essential to accurately predict others' impending actions and flexibly decide whether one should cooperate or compete with them. In evaluation of this function, called mental attribution or theory of mind (ToM) (Premack and Woodruff, 1978), comprehension of reality-incongruent mental states, or false beliefs (FBs), of others is critically important because it generates unique predictions of others' behavior, which are impossible solely from the actual states of the world (Dennett, 1978). Indeed, the ability to pass verbal FB tasks, which is typically acquired at age 4, is considered as a hallmark of ToM acquisition in human development (Wimmer and Perner, 1983). Whether nonhuman animals possess ToM has remained controversial for four decades. Although apes and macaques can predict others' behavior based on understanding of others' knowledge, non-human primates have been believed, until recently, to be deficient in FB attribution (Hare et al., 2001; Kaminski et al., 2008; Krachun et al., 2009). Human neuroimaging studies, such as functional magnetic resonance imaging and positron emission tomography, have revealed activation of a distributed brain network, including the medial prefrontal cortex (mPFC), superior temporal sulcus (STS), and temporoparietal junction (TPJ), in various forms of explicit and implicit ToM tasks (Gallagher and Frith, 2003; Schurz et al., 2014). Nevertheless, the key element of the distributed network playing a causal role in mental attribution remains unidentified, primarily because the capacity to predict others' FB-guided behaviors, a critical prerequisite to ToM (Krupenye and Call, 2019; Premack and Woodruff, 1978; Wimmer and Perner, 1983), has long been believed to be absent in non-human primates (Call and Tomasello, 2008), particularly in macaques (Marticorena et al., 2011; Martin and Santos, 2014).

Despite the lack of evidence for FB attribution, converging evidence indicates the emergence of visual perspective-taking, an ability that is believed to share common cognitive processes with ToM (Hamilton et al., 2009), in macaques. Specifically, macaques follow others' gaze, attribute visual and auditory perceptions to others, and even understand whether food is visible or invisible for conspecifics (de Waal and Ferrari, 2010; Drayton and Santos, 2018; Flombaum and Santos, 2005; Meunier, 2017; Overduin-de Vries et al., 2014; Santos et al., 2006). Furthermore,

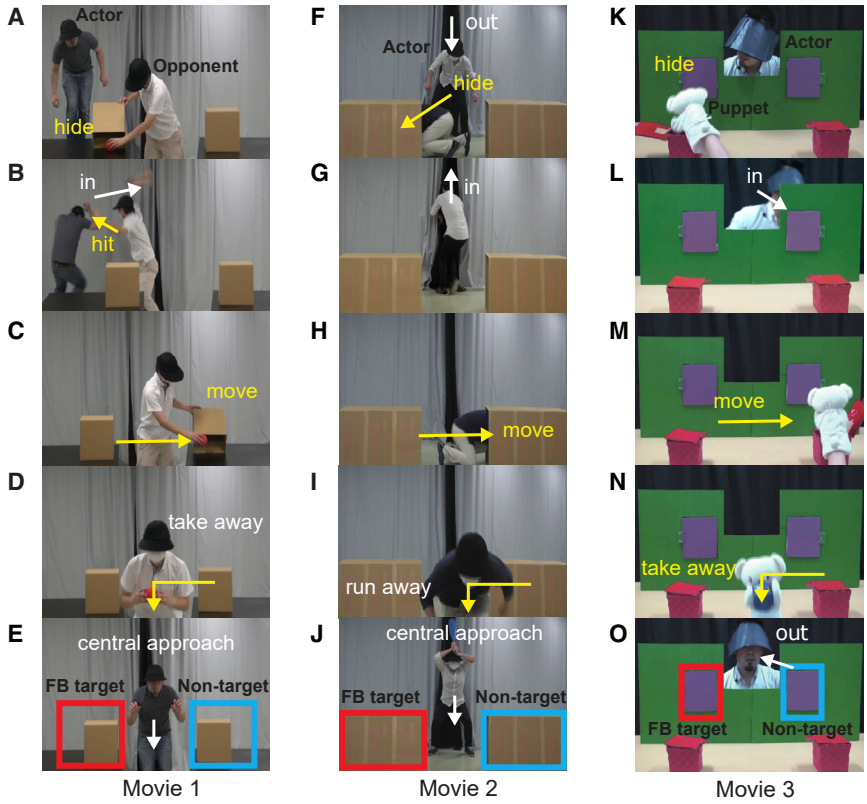

Figure 1. Three Scenarios of False Belief (FB) Test Movies

(A–E) Scenario of FB movie 1.

(F–J) Scenario of FB movie 2.

(K–O) Scenario of FB movie 3. The three scenarios are essentially similar. A human actor pursues a target—a red toy, a human opponent, and a blue toy in movies 1–3, respectively.

(A, F, and K) Initially, the target hides (F) or is hidden (A and K) into one of two boxes.

(B, G, and L) Then, the actor disappears behind the curtain (B and G) or the wall (L).

(C, H, and M) While the actor is absent, the target moves (H) or is moved (C and M) to the opposite box.

(D, I, and N) Subsequently, the target runs away (I) or is taken away (D and N). At this time, the actor's belief (the target must be in one box [FB target]) is dissociated from reality (it is gone).

(E, J, and O) In the FB test phase, the actor reappears, and monkey's spontaneous gaze bias to the FB target (red) over the non-target (blue) is analyzed.

See Figure S2 for alternative scenarios in which the target moves in the presence of the actor during belief induction. Also, see Figure S1 for familiarization movies presented prior to the FB test.

using an anticipatory-looking paradigm (Southgate et al., 2007), a recent study reported that great apes anticipated others' FB-guided actions (Kano et al., 2019; Krupenye et al., 2016). Positive findings indicating FB attribution in apes, coupled with negative findings in macaques, raised the possibility that a basic understanding of FBs evolved uniquely in the hominoid lineage (that includes humans, chimpanzees, bonobos, gorillas, and orangutans) after it diverged from its sister group, the Old World monkeys (the group that includes macaques). The present paper challenged this view by testing in Japanese monkeys (*Macaca fuscata*). If the capacity of FB attribution proves to be present in macaques, then the ability may have evolved in the common ancestor of the Old World monkey and Hominoidea that diverged 30 million years ago. The parallel behaviors of humans and apes, however, are not necessarily accomplished by common neural mechanisms conserved between the species. Thus, a critical question to be asked here is whether FB-attribution-like behaviors of non-human primates originate from functions of homologous neuronal circuits to those of humans. We hypothesize here that the ability to implicitly attribute FBs to others is conserved across many primate species, including humans and macaques, and is supported by homologous neural circuits where the mPFC plays an indispensable role. We focused on the mPFC because neuronal activity in the region can encode others' actions in specific contexts (Haroush and Williams, 2015; Yoshida et al., 2011). To test our hypothesis, we initially introduced an anticipatory-looking FB paradigm to Japanese macaques and evaluated the macaques' ability to comprehend others' FBs. We then chemogenetically blocked (Nagai et al., 2016) neuronal activity in the mPFC to examine whether any behavior indicating implicit FB attribution was specifically altered. The present experimental design is relevant for developing a pioneering animal model to probe the neuronal circuit underlying ToM in non-human primates.

RESULTS

Normal Monkeys' Implicit Gaze Bias Anticipating Other's FB-Guided Behaviors

Spontaneous eye movements of eight normal monkeys were measured with an infrared camera system (Hasegawa et al., 1998; Miyakawa et al., 2018; Nakahara et al., 2016) while they watched movies. We used three movie scenarios (Figures 1A–1O; Videos S1, S2, and S3)—a human actor was competing with another human agent in movies 1 (Figures 1A–1E) and 2 (Figures 1F–1J), whereas the actor witnessed the behavior of a disinterested puppet in movie 3 (Figures 1K–1O). Despite such contextual differences, the plots of the three scenarios were essentially similar. Namely, the actor pursued a particular target that was placed in one of two locations. The target was an apple-like toy in movie 1, the opponent himself in movie 2, and a blue toy in movie 3. Prior to the FB test, a set of familiarization movies (Figures S1A–S1M) were presented, which informed the subject that the target could be placed in either of the boxes and that when the actor knew the true location of the target, he would reach there (Figures S1D, S1H, S1J, and S1M) after lightening up of the boxes or hand windows.

During the belief-induction phase of the FB test movie, the actor saw that the target was initially hidden into one of the boxes (Figures 1A, 1F, and 1K; Figures S2A, S2H, and S2M).

Subsequently, it was moved to the other box while the actor was either absent ("absent switch" [AS] scheme; Figures 1C, 1H, and 1M) or present ("present switch" [PS] scheme; Figures S2B, S2I, and S2N). In any case, the target was finally removed (Figures 1D, 1I, and 1N; Figures S2E, S2K, and S2Q). At this time, the actor's belief that the target used to be in one of the boxes ("FB target" in Figure 1) was dissociated from what the monkey knew to be true (in reality, the target was not present in either box). The actions during the belief induction were inserted to control for several low-level cues—monkeys could not solve the task by simply expecting the actor to look at the first or last hidden box or the last box where the actor attended to.

In the FB test phase, the actor reappeared (Figures 1E, 1J, and 1O; Figures S2F, S2L, and S2R), the boxes or hand windows were lit up for 1 s, and the movie stopped. We analyzed the monkeys' spontaneous gaze during this period from reappearance of the actor until the movie end. If the monkeys anticipated the impending action of the actor based on his FB, then their gaze should have been preferentially biased to the FB target over the other side (or "non-target"). It has been recently suggested that FB attribution might be specifically difficult with the AS scheme in humans (Baillargeon et al., 2018; Dörrenberg et al., 2018; Grosse Wiesmann et al., 2018;Kulke et al., 2018), presumably because the subjects tend to be distracted by the last location in which the subject saw the object regardless of the actor's FB. Thus, we primarily tested with the AS scheme in all monkeys, as in a recent study in apes (Kano et al., 2019), and PS scheme in some additional monkeys. The belief induction scheme (AS versus PS), left-right order, and the scenario types of the FB movie, as well as the number of trials per session in individual animals are summarized in Table 1.

We found two lines of evidence for implicit FB attribution in macaques. First, the monkeys' initial gaze direction was biased to the FB target over the non-target (Figures 2A and 2B), as statistically validated both with mixed-design repeated-measures ANOVA ($F(1, 49) = 11.72$, $p = 0.0013$) and Wilcoxon rank-sum test ($p = 0.022$, $N = 8$). Second, the overall time spent looking in the target area during the test phase was longer than the time spent looking in the non-target area (Figure 2C). Differential looking time score (DLTS), the difference between the target viewing time and the non-target viewing time divided by the sum of them (Senju et al., 2009), was significantly biased to the FB target (Figure 2D; $F(1, 79) = 5.22$, $p = 0.026$). Additionally, we found that the percent fixation time on the movement area of interest (AOI) (Figures S4A–S4C; see STAR Methods) was more than would be expected by an even distribution (Figure S5A; Table S2). Also, we found significant gaze bias (Figure S5B; Table S2) to the hidden target AOI, behind which the actor had been hidden, even in the presence of moving agent or object (Figure S4C; see STAR Methods), indicating the monkey's memory-based gaze bias despite perceptual interference. Taken together, these results indicate that normal macaque monkeys' spontaneous gaze not only tracked moving and hidden objects but also implicitly anticipated the actor's impending actions driven by FBs.

Impairment of FB Attribution by Chemogenetic Neuronal Silencing of mPFC

Next, we found causation between the neuronal activity in the mPFC and the gaze bias toward the FB targets by using a chemogenetic approach (Nagai et al., 2016; Upright et al., 2018). We injected a lentiviral vector (Kato et al., 2011) incorporating hM4Di, an inhibitory DREADD (designer receptor exclusively activated by designer drugs), into the mPFC around medial part of area 9 (9 m) (Petrides and Pandya, 1994) in the left hemisphere in one monkey and bilaterally in four monkeys (Figures 3A and 3B), and immunohistochemically confirmed hM4Di expression in two animals using anti-muscarinic acetylcholine receptor M4 antibody (Figures 3C and 3D). Six weeks following viral injection, we chemogenetically inactivated the mPFC by intramuscular injection of clozapine N-oxide (CNO), a specific ligand to hM4Di. Within 60 to 80 min after CNO injection, when its concentration in the cerebrospinal fluid should reach maximum (Eldridge et al., 2016) and spectral power (Figures 4A and 4B) and peak-to-peak amplitudes (Figures 4A and 4C) of visually evoked potentials significantly decreased in the mPFC (power, $p = 0.0083$; amplitude, $p = 0.0046$; post hoc test with Bonferroni correction), we conducted the behavioral test once again (Videos S1, S2, and S3). Following CNO injection into hM4Di-expressing monkeys (hM4Di(+)CNO(+) condition in Figures 5A–5C, left), the gaze bias to the FB target disappeared both in terms of the first-look ratio ($F(1, 28) = 0.60$, $p = 0.45$) and DLTS ($F(1, 38) = 0.62$, $p = 0.44$) (Table 2). If CNO was injected into animals without hM4Di expression, the first-look ratio ($F(1, 22) = 11.65$, $p = 0.0025$) and DLTS ($F(1, 38) = 5.27$, $p = 0.027$) remained significant (hM4Di(−)CNO(+) condition in Figures 5A–5C, center) (Table 2). In another control condition where saline was injected into hM4Di-expressing animals, the powers and amplitudes of the neural responses were not affected by the injection (Figures 4B and 4C, gray). In this condition, the first-look bias ($F(1, 28) = 12.14$, $p = 0.0016$) and positive DLTS ($F(1, 42) = 4.48$, $p = 0.040$) were significant (hM4Di(+)CNO(−) condition, Figures 5A–5C right) (Table 2). Thus, hM4Di induction or CNO application alone did not alter, but their combination did alter, FB-attribution-like gaze bias of macaques.

The behavioral effect of chemogenetic inhibition could not be ascribed to a generalized decrease in visual attention or deficits of memory-based tracking abilities because the percentage looking time to the moving target AOIs was significantly higher than would be expected by chance ($F(1, 50) = 134.08$, $p = 9.2 \times 10^{-16}$) and the DLTS for hidden targets was significantly positive in the hM4Di(+)CNO(+) condition ($F(1, 12) = 11.27$, $p = 0.0059$) as in the hM4Di(−)CNO(+) (moving target, $F(1, 44) = 337.55$, $p < 2.2 \times 10^{-16}$; hidden target, $F(1, 11) = 5.58$, $p = 0.038$) and hM4Di(+)CNO(−) (moving target, $F(1, 45) = 199.05$, $p < 2.2 \times 10^{-16}$; hidden target, $F(1, 14) = 5.20$, $p = 0.039$) conditions (Figures 5D and 5E) (Table S2). Thus, chemogenetic neuronal silencing of the mPFC specifically eliminated the monkeys' gaze bias to the FB targets while leaving their abilities to track moving and hidden targets intact.

DISCUSSION

In previous studies, FB-attribution-like behaviors have been reportedly deficient in non-human animals other than great apes (Buttelmann et al., 2017; Call and Tomasello, 2008; Krupenye et al., 2016; Marticorena et al., 2011; Martin and Santos, 2014). Contrary to this view, we find spontaneous gaze bias

Table 1. The Order, Protocols, and Neurological Conditions of FB Tests in Individual Animals

Monkey	Session	Trial	Movie	FB Location	Belief Induction Scheme	hM4Di	CNO
T	1	1	2	left	absent switch	–	–
		2	2	right	absent switch	–	–
		3	1	left	absent switch	–	–
		4	1	right	absent switch	–	–
		5	3	left	absent switch	–	–
		6	3	right	absent switch	–	–
	2	1	3	left	absent switch	–	+
		2	2	right	absent switch	–	+
		3	1	left	absent switch	–	+
	3	1	1	left	absent switch	–	+
		2	3	right	absent switch	–	+
		3	2	right	absent switch	–	+
	4	1	2	left	absent switch	+	–
		2	1	left	absent switch	+	–
		3	3	left	absent switch	+	–
	5	1	1	left	absent switch	+	–
		2	3	right	absent switch	+	–
		3	2	right	absent switch	+	–
	6	1	3	right	absent switch	+	+
		2	1	left	absent switch	+	+
		3	2	right	absent switch	+	+
	7	1	3	left	absent switch	+	+
		2	2	left	absent switch	+	+
		3	1	right	absent switch	+	+
P	1	1	2	right	absent switch	–	–
		2	2	left	absent switch	–	–
		3	3	right	absent switch	–	–
		4	3	left	absent switch	–	–
		5	1	right	absent switch	–	–
		6	1	left	absent switch	–	–
	2	1	1	left	present switch	–	–
		2	2	right	present switch	–	–
		3	3	right	present switch	–	–
	3	1	2	left	present switch	–	–
		2	3	left	present switch	–	–
		3	1	right	present switch	–	–
D	1	1	2	left	absent switch	–	–
		2	2	right	absent switch	–	–
		3	1	left	absent switch	–	–
		4	1	right	absent switch	–	–
		5	3	left	absent switch	–	–
		6	3	right	absent switch	–	–
	2	1	1	left	absent switch	–	+
		2	1	right	absent switch	–	+
		3	2	left	absent switch	–	+
		4	2	right	absent switch	–	+
		5	3	left	absent switch	–	+
	2	6	3	right	absent switch	–	+
	3	1	2	left	absent switch	+	+

(*Continued on next page*)

Table 1. *Continued*

Monkey	Session	Trial	Movie	FB Location	Belief Induction Scheme	hM4Di	CNO
D	3	2	1	right	absent switch	+	+
		3	3	left	absent switch	+	+
	4	1	2	right	absent switch	+	+
		2	1	left	absent switch	+	+
		3	3	right	absent switch	+	+
	5	1	2	left	absent switch	+	–
		2	1	right	absent switch	+	–
		3	3	left	absent switch	+	–
		4	2	right	absent switch	+	–
		5	1	left	absent switch	+	–
		6	3	right	absent switch	+	–
F	1	1	2	left	absent switch	–	+
		2	1	right	absent switch	–	+
		3	3	left	absent switch	–	+
	2	1	2	right	absent switch	–	+
		2	1	left	absent switch	–	+
		3	3	right	absent switch	–	+
	3	1	2	right	absent switch	+	–
		2	1	left	absent switch	+	–
		3	3	right	absent switch	+	–
	4	1	3	left	absent switch	+	–
		2	1	right	absent switch	+	–
		3	2	left	absent switch	+	–
	5	1	2	right	absent switch	+	+
		2	1	left	absent switch	+	+
		3	3	right	absent switch	+	+
	6	1	2	left	absent switch	+	+
		2	1	right	absent switch	+	+
		3	3	left	absent switch	+	+
O	1	1	3	left	absent switch	–	–
		2	3	right	absent switch	–	–
		3	2	left	absent switch	–	–
		4	2	right	absent switch	–	–
		5	1	left	absent switch	–	–
		6	1	right	absent switch	–	–
	2	1	3	left	absent switch	+	+
		2	3	right	absent switch	+	+
	3	1	2	left	absent switch	+	+
		2	2	right	absent switch	+	+
		3	1	left	absent switch	+	+
		4	1	right	absent switch	+	+
	4	1	3	left	absent switch	+	–
		2	3	right	absent switch	+	–
		3	2	left	absent switch	+	–
		4	2	right	absent switch	+	–
		5	1	left	absent switch	+	–
		6	1	right	absent switch	+	–

(*Continued on next page*)

Table 1. *Continued*

Monkey	Session	Trial	Movie	FB Location	Belief Induction Scheme	hM4Di	CNO
E	1	1	2	left	absent switch	–	+
		2	1	right	absent switch	–	+
		3	3	left	absent switch	–	+
	2	1	1	left	absent switch	–	+
		2	3	right	absent switch	–	+
E	2	3	2	right	absent switch	–	+
	3	1	1	right	absent switch	+	–
		2	2	left	absent switch	+	–
		3	3	right	absent switch	+	–
	4	1	2	right	absent switch	+	–
		2	1	left	absent switch	+	–
		3	3	left	absent switch	+	–
	5	1	3	right	absent switch	+	+
		2	2	left	absent switch	+	+
		3	1	right	absent switch	+	+
	6	1	1	left	absent switch	+	+
		2	2	right	absent switch	+	+
		3	3	left	absent switch	+	+
S	1	1	2	left	absent switch	–	–
		2	2	right	absent switch	–	–
		3	1	left	absent switch	–	–
		4	1	right	absent switch	–	–
		5	3	left	absent switch	–	–
		6	3	right	absent switch	–	–
V	1	1	3	right	absent switch	–	–
		2	2	right	absent switch	–	–
		3	1	left	absent switch	–	–
	2	1	1	right	absent switch	–	–
		2	3	left	absent switch	–	–
		3	2	left	absent switch	–	–
	3	1	3	left	present switch	–	–
		2	2	left	present switch	–	–
	4	1	2	right	present switch	–	–
		2	3	right	present switch	–	–
	5	1	1	left	present switch	–	–
		2	1	right	present switch	–	–
C	1	1	3	left	absent switch	–	–
		2	3	right	absent switch	–	–
Q	1	1	3	left	absent switch	–	–
		2	3	right	absent switch	–	–

indicating implicit FB attribution in macaque monkeys. Furthermore, although human functional neuroimaging studies reported activation of a distributed brain network, including the mPFC, STS, and TPJ, accompanying FB attribution (Gallagher and Frith, 2003; Schurz et al., 2014), it remains unclear whether individual neural activations are causally linked to FB attribution or simply epiphenomena. By neuronal silencing of the mPFC, one of key loci implicated in both implicit and explicit ToMs in human neuroimaging, we found that the macaques' implicit gaze bias to the FB target can be specifically eliminated while sparing their visually guided and memory-guided tracking abilities. Our macaque model not only provides evidence for FB-attribution-like behaviors in non-hominid primates but also enables to reveal a causal link between neuronal activity in the mPFC and the manifestation of FB-attribution-like behaviors in primates. Thus, it is possible that the sprouting of an ability to implicitly comprehend others'

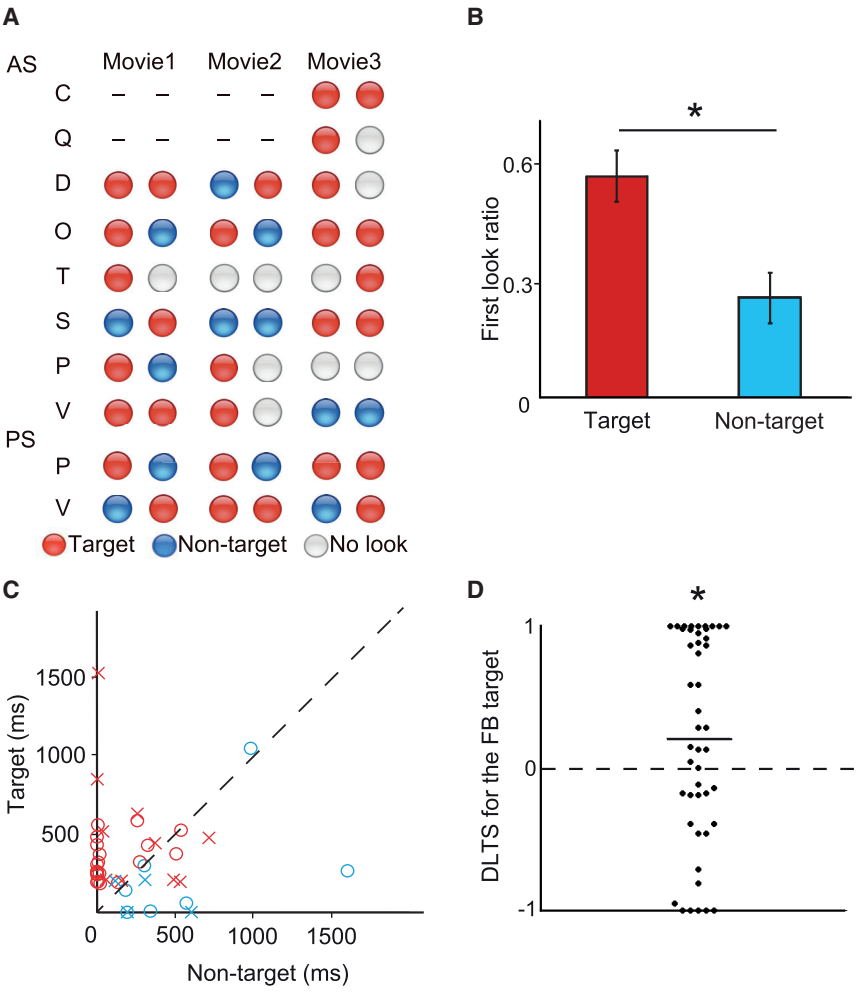

Figure 2. Spontaneous Gaze Bias of Normal Monkeys to the FB Targets

(A) The first-look direction of individual monkeys. Colors indicate initial gaze to the FB target area (red), non-target area (blue), or neither (gray).

(B) Mean ratios of first looks to the target (red) and non-target (blue). Error bar, standard error of the mean (SEM).

(C) Scatterplot of total looking time for the FB target (y axis) and non-target (x axis) for individual trials. Colors indicate initial gaze as in (A). Circles and crosses represent AS type and PS type.

(D) Differential looking time scores (DLTSs) for the FB targets. The horizontal line represents the mean value. Asterisk indicates $p < 0.05$ evaluated with repeated-measures ANOVA.

mental states by neural circuits centered on the mPFC might go back to the ancestry of a primate species common to humans and macaques.

Our paradigms followed the seminal anticipatory-looking FB paradigms in infants and apes (Krupenye et al., 2016; Southgate et al., 2007), excluding the possibility that gaze bias to the FB target was explained by simple strategies expecting that the actor was searching a particular side, the first or last location where the object was hidden, or the last location the actor attended. Because the monkeys' gaze closely tracked the opponent's visible and memorized actions during belief induction (Figures S5A and S5B; Figures 5D and 5E; Videos S1, S2, and S3), it is also not likely that monkeys overlooked the opponent actions and object movements while the actor did not attend (Heyes, 2014). We show combined data from AS-type and PS-type FB tests in Figure 2 because repeated-measures ANOVA revealed neither significant main effects of the belief induction scheme (AS versus PS) (first-look ratio, $F(1, 49) = 1.37$, $p = 0.25$; DLTS, $F(1, 80) = 1.24$, $p = 0.27$) nor significant interactions between the belief induction scheme and the target or non-target factor (first-look ratio, $F(1, 48) = 0.02$, $p = 0.88$; DLTS, $F(1, 78) = 1.26$, $p = 0.27$) (Figures S3A and S3B; Table S1). Post hoc tests confirmed significant first-look bias both in the AS-type ($F(1, 38) = 7.64$, $p = 0.0087$) and PS-type ($F(1, 10) = 5.00$, $p = 0.049$) belief induction schemes, ensuring that the low-level perceptual explanations cannot account for the macaque's first-look bias to the FB target. The DLTS was significantly biased to the FB target in the AS test ($F(1, 64) = 4.62$, $p = 0.036$), but not significantly biased in the PS test ($F(1, 22) = 0.07$, $p = 0.79$), indicating that macaque's initial FB bias might become fragile in the PS condition presumably because the animal's attention might be divided between the FB target and the location the actor attended previously.

It has been speculated that results of implicit FB tests could reflect domain-general submentalizing mechanisms (Heyes, 2014). It should be noted, however, that inanimate control conditions were used in apes to rule out submentalizing as an explanation for primates' FB-based anticipatory looking (Kano et al., 2017; Krupenye et al., 2017). Also, it was argued that non-human primates rely on an innate or learned rule that agents tend to search for things where they last saw them (Perner and Ruffman, 2005), rather than attributing FBs to others. However, this view has been strongly challenged by a recent finding that apes can use a self-experience of learning whether a barrier was opaque or translucent to correctly predict an actor's actions in an anticipatory-looking FB task involving that barrier (Kano et al., 2019).

Positive evidence for macaque's implicit FB attribution with the anticipatory-looking FB paradigm is unexpected because rhesus monkeys (*Macaca mulatta*) tested with a violation-of-expectation paradigm failed to attribute FBs (Marticorena et al., 2011; Martin and Santos, 2014). Three explanations may account for the discrepancy. First, different from human infants, monkeys tested with the violation-of-expectation FB paradigm might be impressed not only by the actor's unexpected action to the non-target but also by the actor's deceived action to the FB target, leading to equivalent looking time. Second, more

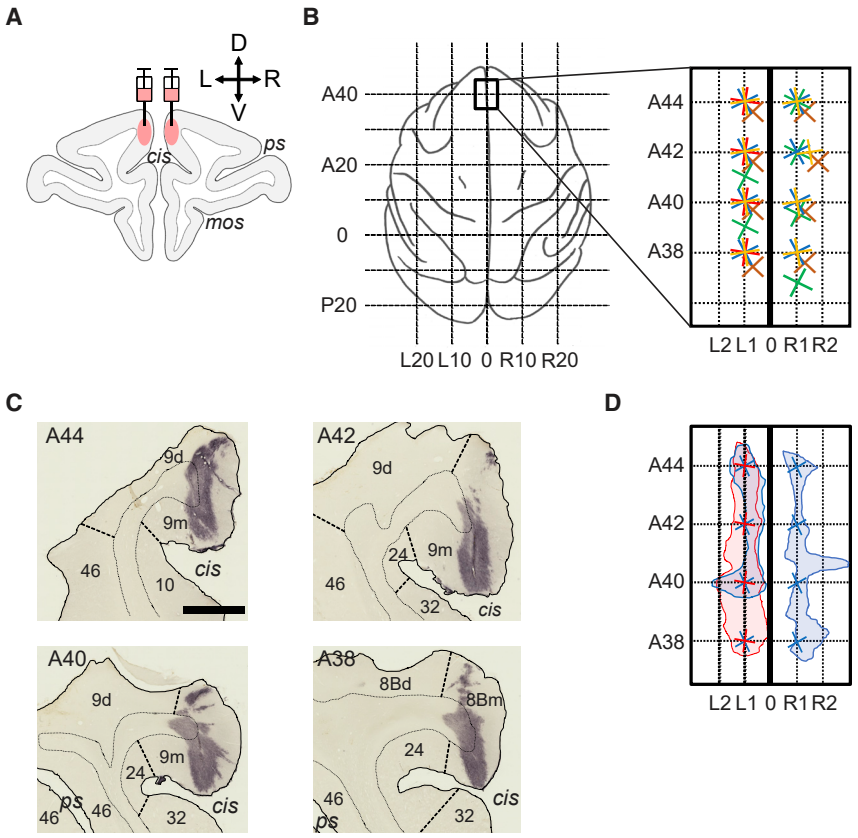

Figure 3. Anatomical Verification of hM4Di Expression in the Medial Prefrontal Cortex (mPFC)

(A) Coronal section of a macaque brain schematically illustrating microinjection of viral vector. R, right; L, left; D, dorsal; V, ventral; *ps*, principal sulcus; *cis*, cingulate sulcus; *mos*, medial orbital sulcus.

(B) Dorsal view of a macaque brain showing antero-posterior (vertical) and medio-lateral (horizontal) stereotaxic coordinates in millimeters. The boxed region is enlarged at right. Different colors indicate injection sites for different monkeys. A, anterior; P, posterior.

(C) Coronal sections of monkey mPFC immunohistochemically stained with an antibody against the hM4Di receptor. Broken and dotted lines express the cytoarchitectonic areal borders and the gray and white matter borders, respectively. Scale bar denotes 2 mm.

(D) Expression of hM4Di reconstructed from the coronal sections of monkeys O (red) and E (blue). Format is as in (B).

subtle bias to the FB target might be detectable with the anticipatory-looking paradigm (Senju et al., 2009; Southgate et al., 2007) where the non-target was empty than with the violation-of-expectation paradigm (Marticorena et al., 2011; Martin and Santos, 2014) where the non-target contained real objects. Third, the discrepancy might be ascribed to different levels of the monkeys' attention because more than half of monkeys were excluded due to disinterest in the prior studies (Marticorena et al., 2011; Martin and Santos, 2014), and the proportion of excluded trials due to "no look" in our study was approximately 20%. In general, participants are highly motivated to attend and predict behavior because of embedding FB content into social dramas that are naturally of high interest and relevance to social animals (Kano et al., 2017). It should be noted that, using the violation-of-expectation FB test, it is difficult to discriminate whether the subjects attribute FBs or just attribute other's ignorance, whereas only those subjects who anticipate others' FB-driven actions should pass the FB test with the anticipatory-looking paradigm (Southgate et al., 2007).

Santos and colleagues demonstrated the macaque's capacity of true belief (TB) attribution with the violation-of-expectation paradigm (Marticorena et al., 2011; Martin and Santos., 2014). Notably, previous studies with anticipatory-looking paradigms in great apes and infants (Krupenye et al., 2016; Senju et al., 2009) reported that all subjects would not necessarily make eye movements predicting the agent's TB-based actions, particularly when they watched novel scenarios. We considered the familiarization trials for movies 1 and 2 as TB condition and tested whether the animals developed TB-attribution-like gaze bias as the number of familiarization trials increased using Spearman's rank correlation test (Figures S6A and S6B). We found that the animals' gaze became significantly biased to the TB target across sessions, both in terms of the first-look direction ($\rho = 0.65$, $p = 0.043$) and looking time ($\rho = 0.23$, $p = 0.018$). Taken together, it is likely that macaques may implicitly attribute TBs to others but that it takes some familiarization before they prospectively anticipate an agent's TB-guided behaviors.

We repeatedly presented three types of movie scenarios to obtain a statistically sufficient number of trials while reducing the total number of animals used. However, the gaze bias to the FB target should not be ascribed to possible learning effects for two reasons. First, analyses using only the first trials of each scenario (Figures S7A and S7B) confirmed significant bias of both the first-look direction (Wilcoxon rank-sum test, $p = 0.013$) and DLTS ($F(1, 20) = 110.26$, $p = 0.024$) toward the FB targets. Second, no significant trends with increasing the number of repetitions was observed in the first-look score (Figure S7C) or DLTS (Figure S7D). Also, we have evaluated the effect of trial repetition by conducting repeated-measures ANOVA in two individual monkeys (D and T) who initially underwent FB tests in the hM4Di(−)CNO(−) condition and subsequently in the hM4Di(−)CNO(+) condition. Although the number of samples is very small, the analysis shows that first-look bias to the FB target remained significant ($F(1, 9) = 5.58$, $p = 0.044$) even on the second trial. Although DLTS was above zero (looking time was longer for the FB target) on the second trial, it did not reach significance ($F(1, 16) = 2.48$, $p = 0.14$), presumably due to the small sample size. Together with the analysis showing no significant effects of trial repetition in the combined data (Figures S7C and S7D),

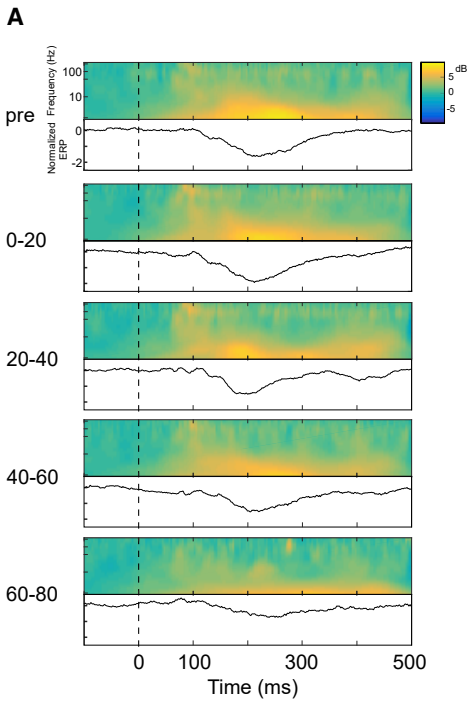

Figure 4. Chemogenetic Suppression of Neuronal Activity in the mPFC

(A) Event-related spectral perturbation (ERSP; top) and normalized event-related potential (ERP; bottom) in the mPFC during movie presentations before CNO injection (pre, −20–0), and 0–20, 20–40, 40–60, and 60–80 min after injection. Color scale bar on top right indicates spectral power ratio normalized by pre-stimulation power.

(B) Normalized visually evoked power plotted against the time after CNO (black) and saline (gray) injection. Double asterisk indicates $p < 0.01$ evaluated with post hoc Bonferroni pairwise comparison.

(C) Normalized peak-to-peak amplitude of visually evoked potentials plotted against the time after CNO injection. CNO (black) and saline (gray) injection.

these results suggest that decreased performance on FB tests after chemogenetic silencing might not be simply explained by the habituation effect. To control motivation for performing the movie-watching task, monkeys received juice at the end of each trial. Juice supply was just linked to the end of movie, not with specific gaze positions. More importantly, Figure S7 revealed no significant effects of trial repetition on the first-look ratio or DLTS, indicating that the monkeys' gaze bias to the FB target was neither reinforced nor habituated by the juice supply.

The fixed order of presentation of the familiarization trials or the animal's intrinsic side bias, if any, might have affected the animal's gaze behavior. To rule out these possibilities, we analyzed the animal's gaze behavior with repeated-measures ANOVA, taking the effect of the location (left versus right) of the FB target into account, which revealed no main effects of the target location on the first-look ratio ($F(1, 204) = 0.37$, $p = 0.54$) or DLTS ($F(1, 82) = 0.03$, $p = 0.87$) (Table S3). Also, no interactions were found between the target location and the first-look ratio ($F(1, 203) = 0.00$, $p = 1.0$) or DLTS ($F(1, 82) = 0.03$, $p = 0.087$). These results suggest that the fixed order of familiarization movies did not significantly affect the animal's gaze bias to the FB target.

We examined the sex factor (male versus female) with repeated-measure ANOVA (Table S4), which revealed neither significant effects of the sex factor on the first-look ratio ($F(1, 38) = 0.69$, $p = 0.41$) and DLTS ($F(1, 29) = 0.82$, $p = 0.37$) nor their interaction with the FB target or non-target factor (first-look ratio, $F(1, 36) = 0.30$, $p = 0.59$; DLTS, $F(1, 58) = 0.82$, $p = 0.37$).

CNO was reverse-metabolized into clozapine in rodents *in vivo* (Gomez et al., 2017). However, the concentration of clozapine in cerebrospinal fluid at the same dose of the current admistration (3 mg/kg CNO) has been reported to be negligibly low to cause off-target effects in macaques (Nagai et al., 2016). Moreover, systemic CNO administration in our study did not produce any task impairment before hM4Di induction but did induce cognitive deficits in the same animals after hM4Di induction. Therefore, the cognitive deficits observed in the hM4Di(+)CNO(+) condition could not be ascribed to the effects of CNO administration alone.

One out of 5 animals that underwent chemogenetic inhibition received a unilateral injection, whereas the remaining 4 received bilateral injections of the lentivirus. We conducted repeated-measures ANOVA, which revealed neither main effects of the laterality of hM4Di injection (unilateral injection versus bilateral injection) on the first-look ratio ($F(1, 28) = 0.02$, $p = 0.90$) and DLTS ($F(1, 24) = 0.10$, $p = 0.76$) nor their interaction with the FB target or non-target factor (first-look ratio, $F(1, 26) = 0.08$, $p = 0.38$; DLTS, $F(1, 50) = 0.03$, $p = 0.86$). Notably, for those that underwent a bilateral injection, the gaze bias to the FB target disappeared both in terms of the first-look direction ($F(1, 22) = 0.08$, $p = 0.77$) and DLTS ($F(1, 42) = 0.05$, $p = 0.81$).

Although we included "no look" trials in the analysis of first-look ratios following the previous research (Krupenye et al., 2016), the first-look proportion, defined as the number of trials on which the participant made a correct first look divided by the number of trials on which the participant made a first look (correct or incorrect), was also significantly above chance in hM4Di(−)CNO(−) ($p = 0.020$), hM4Di(−)CNO(+) ($p = 0.012$), and hM4Di(+)CNO(−) ($p = 0.017$) conditions but not in the hM4Di(+)CNO(+) condition ($p = 0.66$).

We have conducted a permutation test to examine whether the first-look bias (the differential first-look ratio between the target and non-target) and the DLTS were significantly different across conditions. The first-look bias was significantly different ($p = 0.036$) between the hM4Di(−)CNO(+) and hM4Di(+)CNO(+) conditions in the 4 animals (D, T, F, and E) that underwent the FB test under both conditions. When the hM4Di(+)CNO(+) condition was compared with all three control conditions—hM4Di(−)CNO(−), hM4Di(−)CNO(+), and hM4Di(+)CNO(−)—combined together, yhe difference of the first-look bias between the hM4Di(+)CNO(+) and control conditions was marginally

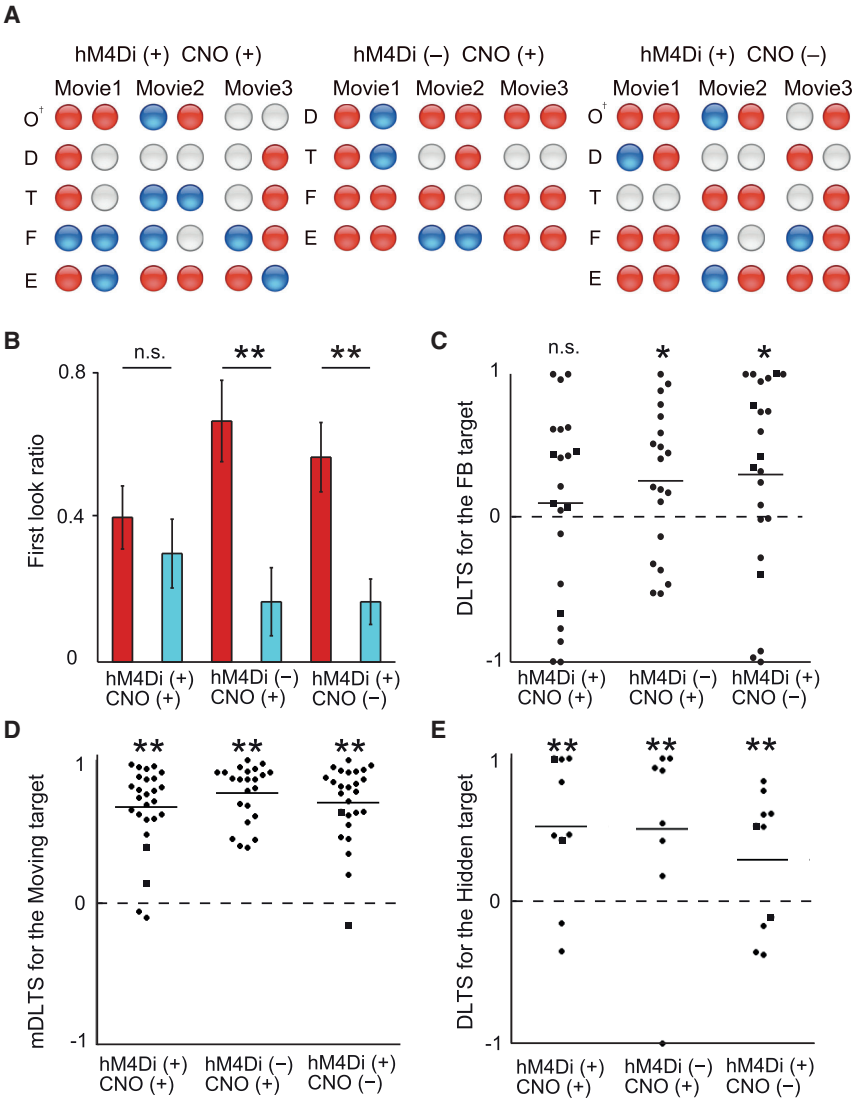

Figure 5. Chemogenetic Silencing of mPFC Neurons Specifically Impaired FB Comprehension

(A) The first look to the FB target (red), non-target (blue), or neither (gray) in hM4Di(+)CNO(+) (left), hM4Di(−)CNO(+) (center), and hM4Di(+)CNO(−) (right) conditions, respectively. Dagger represents a monkey with unilateral hM4Di injection.

(B) Ratio of the first look to the FB target (red) and non-target (blue) in each condition.

(C) DLTS for the FB targets in each condition. Dots and squares represent data from monkeys with bilateral and unilateral hM4Di injection, respectively.

(D) Modified DLTS (mDLTS) for the moving targets in each condition.

(E) DLTS for the hidden targets in each condition. (D) and (E) included data from "no look" trials. Formats are as in Figure 2.

significant ($p = 0.051$). However, the DLTS was not significantly different, either between the hM4Di(−)CNO(+) and hM4Di(+)CNO(+) conditions ($p = 0.19$), or between the hM4Di(+)CNO(+) and all three control conditions ($p = 0.15$). Thus, chemogenetic neuronal manipulation in the mPFC impaired FB-attribution-like behavior, particularly the first-look bias, following the AS-scheme belief induction. The most parsimonious interpretation of these results is that mPFC inactivation impairs the initial gaze bias to the FB target at least when the FB target is dissociated from the last location of the target remembered by the monkeys.

Neurophysiological studies showed that mPFC contains single neurons specifically distinguishing behaviors of self and others in some social contexts (Haroush and Williams, 2015; Yoshida et al., 2011), which provides further evidence supporting that the behaviors affected by mPFC suppression would be related to domain-specific social cognitive processes rather than domain-general submentalizing processes.

Because social disability due to impaired development of ToM is one of the core symptoms of major psychiatric disorders, such as autism and schizophrenia (Frith, 2001), elucidating the neural basis of ToM is indispensable not only for exploring the biological origin of our social intelligence but also for clarifying the pathology of these psychiatric disorders. It has been debated whether infants or non-human primates possess just belief-like states or full-blown belief representation as flexible as human adults (Butterfill and Apperly, 2013). It would be important to explore in the future what exactly infants and non-human primates can represent in an FB task by comparative psychological and neuroscientific approaches. Causation between neuronal activity in a particular cortical site and cognitive behavior is difficult to prove solely by non-invasive imaging approaches. Specifically, there still remains controversy about the causal role of mPFC in ToM in human neuroimaging and neuropsychology studies (Bird et al., 2004), justifying the need to examine its causal role in FB-attribution-like behaviors by using an appropriate non-human primate animal model under controlled experimental setups. The present study has opened a way to chemogenitically test the causal role of neuronal inputs to particular brain regions implicated in ToM in macaque monkeys, which is an experimental model animal closest to humans among those used in neuroscience research.

STAR★METHODS

Detailed methods are provided in the online version of this paper and include the following:

Table 2. Significance of Gaze Bias to the False Belief Targets in Different Conditions Evaluated with Repeated-Measures ANOVA

	hM4Di(+)CNO(+)			hM4Di(−)CNO(+)			hM4Di(+)CNO(−)		
Parameter	*F*	*df*	*P*	*F*	*df*	*P*	*F*	*df*	*P*
First-look ratio	0.60	1, 28	0.45	11.65	1, 22	0.0025	12.14	1, 28	0.0016
Differential looking time score	0.62	1, 38	0.44	5.27	1, 38	0.027	4.48	1, 42	0.040

- KEY RESOURCES TABLE
- LEAD CONTACT AND MATERIALS AVAILABILITY
- EXPERIMENTAL MODEL AND SUBJECT DETAILS
  - Animal care and use
- METHOD DETAILS
  - Experimental schedule
  - Behavioral preparations
  - False belief test
  - Behavioral data analysis
  - Evaluation of low level abilities
  - Viral vector preparation
  - Surgery
  - Drug administration
  - Electrophysiological recording *in vivo*
  - Histology
- QUANTIFICATION AND STATISTICAL ANALYSIS
- DATA AND CODE AVAILABILITY

SUPPLEMENTAL INFORMATION

Supplemental Information can be found online at https://doi.org/10.1016/j.celrep.2020.03.013.

ACKNOWLEDGMENTS

We thank T. Watanabe and R. Sato for assistance; Meno for illustration; and R. Ohashi, K. Oyachi, and Y. Ajioka for technical comments on histology. Financial support was provided by the Japan Society for the Promotion of Science (grants KAKENHI 26293261 to T.S., KAKENHI 26242088 to I.H., KAKENHI 15H05919 and 16K01959 to K. Kawasaki, KAKENHI JP15H05917 to T.M., and KAKENHI 19K17106 to T.H.); Ministry of Education, Culture, Sports, Science and Technology (grant 156180-510210); Merck Sharp and Dohme (grant J11F0765 to T.S.); and by AMED (grant number JP18dm0107146 to T.M.).

AUTHOR CONTRIBUTIONS

T.H., J.E., K. Kawasaki, R.A., A.I., T.S., and I.H. designed experiments. T.H., R.A., and K. Kawasaki performed behavioral experiments and analyzed the data. T.H., R.A., K. Kawasaki, T.M., and Y.N. performed the DREADD injection. K. Kobayashi and S.K. prepared viral vector constructs. R.A., K. Kawasaki, T.M., and Y.H. performed histology. R.A. and K. Kawasaki acquired and analyzed neuronal data. T.H., R.A., K. Kawasaki, J.E., and I.H. wrote the manuscript.

DECLARATION OF INTERESTS

All authors declare no competing financial interests.

Received: August 1, 2019
Revised: December 23, 2019
Accepted: March 5, 2020
Published: March 31, 2020

REFERENCES

Baillargeon, R., Buttelmann, D., and Southgate, V. (2018). Invited commentary: Interpreting failed replications of early false-belief findings: Methodological and theoretical considerations. Cogn. Dev. *46*, 112–124.

Bird, C.M., Castelli, F., Malik, O., Frith, U., and Husain, M. (2004). The impact of extensive medial frontal lobe damage on 'Theory of Mind' and cognition. Brain *127*, 914–928.

Buttelmann, D., Buttelmann, F., Carpenter, M., Call, J., and Tomasello, M. (2017). Great apes distinguish true from false beliefs in an interactive helping task. PLoS One *12*, e0173793.

Butterfill, S.A., and Apperly, I.A. (2013). How to construct a minimal Theory of Mind. Mind Lang. *28*, 606–637.

Call, J., and Tomasello, M. (2008). Does the chimpanzee have a theory of mind? 30 years later. Trends Cogn. Sci. *12*, 187–192.

de Waal, F.B., and Ferrari, P.F. (2010). Towards a bottom-up perspective on animal and human cognition. Trends Cogn. Sci. *14*, 201–207.

Dennett, D.C. (1978). Beliefs about beliefs. Behav. Brain Sci. *1*, 568–570.

Dörrenberg, S., Rakoczy, H., and Liszkowski, U. (2018). How (not) to measure infant theory of mind: Testing the replicability and validity of four non-verbal measures. Cogn. Dev. *46*, 12–30.

Drayton, L.A., and Santos, L.R. (2018). What do monkeys know about others' knowledge? Cognition *170*, 201–208.

Eldridge, M.A., Lerchner, W., Saunders, R.C., Kaneko, H., Krausz, K.W., Gonzalez, F.J., Ji, B., Higuchi, M., Minamimoto, T., and Richmond, B.J. (2016). Chemogenetic disconnection of monkey orbitofrontal and rhinal cortex reversibly disrupts reward value. Nat. Neurosci. *19*, 37–39.

Flombaum, J.I., and Santos, L.R. (2005). Rhesus monkeys attribute perceptions to others. Curr. Biol. *15*, 447–452.

Frith, U. (2001). Mind blindness and the brain in autism. Neuron *32*, 969–979.

Gallagher, H.L., and Frith, C.D. (2003). Functional imaging of 'theory of mind'. Trends Cogn. Sci. *7*, 77–83.

Gomez, J.L., Bonaventura, J., Lesniak, W., Mathews, W.B., Sysa-Shah, P., Rodriguez, L.A., Ellis, R.J., Richie, C.T., Harvey, B.K., Dannals, R.F., et al. (2017). Chemogenetics revealed: DREADD occupancy and activation via converted clozapine. Science *357*, 503–507.

Grosse Wiesmann, C., Friederici, A.D., Disla, D., Steinbeis, N., and Singer, T. (2018). Longitudinal evidence for 4-year-olds' but not 2- and 3-year-olds' false belief-related action anticipation. Cogn. Dev. *46*, 58–68.

Hamilton, A.F., Brindley, R., and Frith, U. (2009). Visual perspective taking impairment in children with autistic spectrum disorder. Cognition *113*, 37–44.

Hare, B., Call, J., and Tomasello, M. (2001). Do chimpanzees know what conspecifics know? Anim. Behav. *61*, 139–151.

Haroush, K., and Williams, Z.M. (2015). Neuronal prediction of opponent's behavior during cooperative social interchange in primates. Cell *160*, 1233–1245.

Hasegawa, I., Fukushima, T., Ihara, T., and Miyashita, Y. (1998). Callosal window between prefrontal cortices: cognitive interaction to retrieve long-term memory. Science *281*, 814–818.

Heyes, C. (2014). False belief in infancy: a fresh look. Dev. Sci. *17*, 647–659.

Kaminski, J., Call, J., and Tomasello, M. (2008). Chimpanzees know what others know, but not what they believe. Cognition *109*, 224–234.

Kano, F., Krupenye, C., Hirata, S., and Call, J. (2017). Eye tracking uncovered great apes' ability to anticipate that other individuals will act according to false beliefs. Commun. Integr. Biol. *10*, e1299836.

Kano, F., Krupenye, C., Hirata, S., Tomonaga, M., and Call, J. (2019). Great apes use self-experience to anticipate an agent's action in a false-belief test. Proc. Natl. Acad. Sci. USA *116*, 20904–20909.

Kato, S., Kobayashi, K., Inoue, K., Kuramochi, M., Okada, T., Yaginuma, H., Morimoto, K., Shimada, T., Takada, M., and Kobayashi, K. (2011). A lentiviral strategy for highly efficient retrograde gene transfer by pseudotyping with fusion envelope glycoprotein. Hum. Gene Ther. *22*, 197–206.

Krachun, C., Carpenter, M., Call, J., and Tomasello, M. (2009). A competitive nonverbal false belief task for children and apes. Dev. Sci. *12*, 521–535.

Krupenye, C., and Call, J. (2019). Theory of mind in animals: Current and future directions. Wiley Interdiscip. Rev. Cogn. Sci. *10*, e1503.

Krupenye, C., Kano, F., Hirata, S., Call, J., and Tomasello, M. (2016). Great apes anticipate that other individuals will act according to false beliefs. Science *354*, 110–114.

Krupenye, C., Kano, F., Hirata, S., Call, J., and Tomasello, M. (2017). A test of the submentalizing hypothesis: Apes' performance in a false belief task inanimate control. Commun. Integr. Biol. *10*, e1343771.

Kulke, L., von Duhn, B., Schneider, D., and Rakoczy, H. (2018). Is Implicit Theory of Mind a Real and Robust Phenomenon? Results From a Systematic Replication Study. Psychol. Sci. *29*, 888–900.

Marticorena, D.C., Ruiz, A.M., Mukerji, C., Goddu, A., and Santos, L.R. (2011). Monkeys represent others' knowledge but not their beliefs. Dev. Sci. *14*, 1406–1416.

Martin, A., and Santos, L.R. (2014). The origins of belief representation: monkeys fail to automatically represent others' beliefs. Cognition *130*, 300–308.

Meunier, H. (2017). Do monkeys have a theory of mind? How to answer the question? Neurosci. Biobehav. Rev. *82*, 110–123.

Miyakawa, N., Majima, K., Sawahata, H., Kawasaki, K., Matsuo, T., Kotake, N., Suzuki, T., Kamitani, Y., and Hasegawa, I. (2018). Heterogeneous Redistribution of Facial Subcategory Information Within and Outside the Face-Selective Domain in Primate Inferior Temporal Cortex. Cereb. Cortex *28*, 1416–1431.

Nagai, Y., Kikuchi, E., Lerchner, W., Inoue, K.I., Ji, B., Eldridge, M.A., Kaneko, H., Kimura, Y., Oh-Nishi, A., Hori, Y., et al. (2016). PET imaging-guided chemogenetic silencing reveals a critical role of primate rostromedial caudate in reward evaluation. Nat. Commun. *7*, 13605.

Nakahara, K., Adachi, K., Kawasaki, K., Matsuo, T., Sawahata, H., Majima, K., Takeda, M., Sugiyama, S., Nakata, R., Iijima, A., et al. (2016). Associative-memory representations emerge as shared spatial patterns of theta activity spanning the primate temporal cortex. Nat. Commun. *7*, 11827.

Overduin-de Vries, A.M., Spruijt, B.M., and Sterck, E.H. (2014). Long-tailed macaques (Macaca fascicularis) understand what conspecifics can see in a competitive situation. Anim. Cogn. *17*, 77–84.

Perner, J., and Ruffman, T. (2005). Psychology. Infants' insight into the mind: how deep? Science *308*, 214–216.

Petrides, M., and Pandya, D.N. (1994). Handbook of Neuropsychology, *Volume 9* (Elsevier).

Premack, D., and Woodruff, G. (1978). Does the chimpanzee have a theory of mind? Behav. Brain Sci. *4*, 515–526.

Saleem, K., and Logothetis, N. (2012). A Combined MRI and Histology Atlas of the Rhesus Monkey Brain in Stereotaxic Coordinates (Elsevier).

Santos, L.R., Nissen, A.G., and Ferrugia, J.A. (2006). Rhesus monkeys, *Macaca mulatta*, know what others can and cannot hear. Animal Behaviour *71*, 1175–1181.

Schurz, M., Radua, J., Aichhorn, M., Richlan, F., and Perner, J. (2014). Fractionating theory of mind: a meta-analysis of functional brain imaging studies. Neurosci. Biobehav. Rev. *42*, 9–34.

Senju, A., Southgate, V., White, S., and Frith, U. (2009). Mindblind eyes: an absence of spontaneous theory of mind in Asperger syndrome. Science *325*, 883–885.

Southgate, V., Senju, A., and Csibra, G. (2007). Action anticipation through attribution of false belief by 2-year-olds. Psychol. Sci. *18*, 587–592.

Upright, N.A., Brookshire, S.W., Schnebelen, W., Damatac, C.G., Hof, P.R., Browning, P.G.F., Croxson, P.L., Rudebeck, P.H., and Baxter, M.G. (2018). Behavioral Effect of Chemogenetic Inhibition Is Directly Related to Receptor Transduction Levels in Rhesus Monkeys. J. Neurosci. *38*, 7969–7975.

Wakaizumi, K., Kondo, T., Hamada, Y., Narita, M., Kawabe, R., Narita, H., Watanabe, M., Kato, S., Senba, E., Kobayashi, K., et al. (2016). Involvement of mesolimbic dopaminergic network in neuropathic pain relief by treadmill exercise: A study for specific neural control with Gi-DREADD in mice. Mol. Pain *12*, 1744806916681567.

Walker, A.E. (1940). A cytoarchitectural study of the prefrontal area of the macaque monkey. J. Comp. Neurol. *73*, 59–86.

Wimmer, H., and Perner, J. (1983). Beliefs about beliefs: representation and constraining function of wrong beliefs in young children's understanding of deception. Cognition *13*, 103–128.

Yoshida, K., Saito, N., Iriki, A., and Isoda, M. (2011). Representation of others' action by neurons in monkey medial frontal cortex. Curr. Biol. *21*, 249–253.

STAR★METHODS

KEY RESOURCES TABLE

REAGENT or RESOURCE	SOURCE	IDENTIFIER
Antibodies		
Anti-muscarinic acetylcholine receptor M4 antibody(rabbit)	Santa cruz biotechnology	Cat# sc-9109; RRID: AB_2080211
Anti-muscarinic acetylcholine receptor M4 antibody(mouse)	Millipore	Cat# MAB1576; RRIS: AB_2080217
Anti-rabbit IgG antibody	Jackson ImmunoResearch Labs	Cat# 711-065-152; RRID: AB_2340593
Anti-mouse IgG antibody	Jackson ImmunoResearch Labs	Cat# 715-065-150; RRID: AB_2307438
Bacterial and Virus Strains		
FuG-B2-hM4D-WPRE	Department of Molecular Genetics, Institute of Biomedical Sciences, Fukushima Medical University, Fukushima, Japan	N/A
Chemicals, Peptides, and Recombinant Proteins		
Clozapine-N-oxide	Toronto Research, Toronto, Canada	Cat# C587520
Cresyl violet	Acros, Geel, Belgium	Cat# 10510-54-0
Experimental Models: Organisms/Strains		
Japanese macaque (*Macaca fuscata*)	National BioResource Project "Japanese Monkeys" by the Ministry of Education, Culture, Sports, Science and Technology (MEXT) Japan	https://nihonzaru.jp/aboutus_2_e.html
Software and Algorithms		
MATLAB	Mathworks	https://www.mathworks.com/
R	R Foundation for Statistical Computing	https://www.r-project.org/
EEGLAB	Swartz Center for Computational Neuroscience at the University of California San Diego	https://sccn.ucsd.edu/eeglab/index.php
Free-D	Institut National de la Recherche Agronomique	http://free-d.versailles.inra.fr/#features
Other		
Microelectrodes	FHC	https://www.fh-co.com/

LEAD CONTACT AND MATERIALS AVAILABILITY

Further information and requests for resources and reagents should be directed to and will be fulfilled by the Lead Contact, Isao Hasegawa (ihasegawa-nsu@umin.ac.jp). This study did not generate new unique reagents.

EXPERIMENTAL MODEL AND SUBJECT DETAILS

Animal care and use

A total of 10 Japanese monkeys (*Macaca fuscata*) (6 male and 4 female, body weight 4.5–9.0 kg, age 4–10 years old), provided by the National BioResource Project "Japanese Monkeys" by the Ministry of Education, Culture, Sports, Science and Technology (MEXT) Japan, were used in the study. All monkeys were housed in standard primate cages in an air-conditioned room under a 14/10-h light-dark cycle with environmental enrichment that allowed them to live comfortably. The monkeys were given primate food supplemented with fruits and vegetables. Animal housing, experimental protocols, and procedures for amelioration of suffering conformed to the Act on Welfare and Management of Animals in Japan, Fundamental Guidelines for Proper Conduct of Animal Experiment and Related Activities in Academic Research Institutions under the jurisdiction of the MEXT Japan, and the National Institute of Health Guide for the Care and Use of Laboratory Animals.

METHOD DETAILS

Experimental schedule

The experimental protocols were approved by the Institutional Animal Care and Use Committee (Permission number 28-345) and Gene Modification Experiments Safety Committee (Permission number SD00719) of Niigata University.

In the first part of the study, we introduced the anticipatory looking false belief (FB) paradigm (Krupenye et al., 2016; Southgate et al., 2007) in 8 normal monkeys (C, Q, D, O, T, S, P, V). In the second part, we examined the causal role of the medial prefrontal cortex (mPFC) in implicit FB recognition by chemogenetic deactivation experiments in 5 monkeys (O, D, T, F, E) with a combination of hM4Di, an inhibitory designer receptor exclusively activated by designer drugs (DREADD), and its specific ligand, clozapine-N-oxide (CNO). To examine the reverse-metabolized effect of CNO into clozapine, prior to hM4Di induction, the FB test was done with intramuscular injection of CNO (hM4Di(−)CNO(+) condition) in 4 monkeys (D, T, E, F).

Six weeks following injection of the hM4Di-incorporating vector in the mPFC, five animals (O, D, T, F, E) underwent FB tests either with intramuscular application of CNO (hM4Di(+)CNO(+) condition) or saline (hM4Di(+)CNO(−) condition). The order of application of CNO and saline was counterbalanced across monkeys.

The order of movie presentations and the number of trials per session for each animal is showed in Table 1.

Behavioral preparations

At the start of the study, 6 of the 10 monkeys (C, Q, O, P, S, V) had experienced a visual fixation task for other projects. The other 4 monkeys (D, T, E, F), specifically designated for the present study, were trained in the fixation task as previously described (Hasegawa et al., 1998; Miyakawa et al., 2018; Nakahara et al., 2016). For calibration, monkeys were required to maintain their gaze to 9 white spots (0.3°) placed on 4 corners, in the middle of 4 corners, and a center of square that is the same size of movies used in tests. Briefly, monkeys were required to maintain their gaze within a window of 1–3° in visual angle centered on a white spot (0.3°) presented on a 22-inch LCD monitor (BenQ, XL 2411 T, Taipei, Taiwan) with a viewing angle of 30° × 20° at a distance of 50 cm, and a refresh rate of 100 Hz. The monkey sat comfortably on a primate chair (Vivo, Hokkaido, Japan) with head position maintained with a custom-made non-invasive head guard made of dental acrylic or a titanium head holder (Gray Matter Research, MT, USA). Eye positions of the animal were non-invasively captured and calibrated with an infrared camera system at a sampling rate of 300 Hz (irec_2HS, https://staff.aist.go.jp/k.matsuda/eye/). Task control and data acquisition were done with custom-made software (NSCS, Niigata, Japan) and PCI eXtensions for Instrumentation (PXI) running on a Real-Time LabVIEW system (National Instruments, TX, USA). Movies were presented with visual stimulation software (ActiveSTIM, http://www.danko-nikolic.com/activestim/) synchronized with the PXI system. Eye position data were sampled at 1 kHz with the system.

Prior to the FB test, eight monkeys were habituated in a movie-viewing task with movies depicting inanimate objects and animated objects displaying simple articulated motions. The habituation trial started when the monkey pulled a lever. Following stable fixation for 0.5 s, a movie was presented on the display. The monkey was allowed to freely watch the movie. However, if the monkey's gaze went outside of the display, the trial was aborted. If the monkey released the lever within 1 s after the end of the movie, the monkey obtained a drop of fruit juice as reward. The maximum duration of the habituation movies was 40 s for two monkeys (P, V), 30 s for four monkeys (T, D, E, F) and 5 s for two monkeys (C, O). The remaining two monkeys (S, Q) were not habituated in the movie-viewing task. We skipped or shortened habituation training in several monkeys when these monkeys had already been habituated to the fixation task and their gaze did not avert from the display for several trial.

False belief test

In the FB test session, eye positions of the animals were measured while they watched a set of familiarization movies and FB test movies. The interval between the familiarization movie and the test movie or two familiarization movies was approximately 20 s. Inter-session interval was 2 days or longer. The familiarization/FB test trials were conducted as in the aforementioned movie-viewing trials, except that the trials were not aborted even when the monkey's gaze went out of the display. We prepared three different scenarios of motion pictures (Figures 1A–1O; Figures S1A–S1M and S2A–S2R; see also Videos S1, S2, and S3) taken with a video camera (HDR-CX560V, Sony, Tokyo, Japan) and edited with Adobe Aftereffect (Adobe, CA, USA). We initially tested two monkeys (C, Q) with a scenario (Movie 3), and subsequently tested eight monkeys (D, O, T, S, P, V, E, F) with all three scenarios (Figures 2A and 5A). The presentation order of the scenario types and conditions were counter-balanced across subjects. We used three scenarios to examine monkeys' anticipatory oculomotor responses in different contexts—a human actor was competing with another human agent in Movies 1 and 2, whereas the actor witnessed the behavior of a disinterested puppet in Movie 3. Despite these contextual differences, the plots of the three scenarios were essentially similar. Namely, the actor pursued a particular target that was placed in one of two locations. The target was an apple-like toy in Movie 1 (Figures 1A–1E), the opponent himself in Movie 2 (Figures 1F–1J), and a blue toy in Movie 3 (Figures 1K–1O). Prior to the FB test, a set of familiarization movies were presented. In the first part of the familiarization (familiarization 1) in Movie 3, the actor reached a visible target on one of the boxes after the hand windows were lit up (Figures S1I and S1J). In the main part of the familiarization (Figures S1C and S1G), or familiarization 2 in Movie 3 (Figure S1L), the actor witnessed the target hidden in one of the boxes. After the lightening up of the boxes or hand windows, the actor correctly reached the target (Figures S1D, S1H, and S1M). These familiarization movies let the subject know that when the actor knew the true location of target, the actor would reach there. The right-target and left-target movies were repeatedly presented to ensure

that the target could be placed in either of the boxes. During the belief-induction phase of the FB test movie, the actor saw that the target was initially hidden into one of the boxes (Figures 1A, 1F, and 1K; Figures S2A, S2H, and S2M). Subsequently, it was moved to the other box while the actor was either absent (AS-scheme; Figures 1C, 1H, and 1M) or present (PS-scheme; Figures S2B, S2H, and S2N). In any case, the target was finally removed (Figures 1D, 1I, and 1N; Figures S2E, S2K, and S2Q). In the FB test phase, the actor reappeared (Figures 1E, 1J, and 1O; Figures S2F, S2L, and S2R), the boxes or hand windows were lit up for 1 s, and the movie stopped. We analyzed the monkey's spontaneous gaze during this period from reappearance of the actor till the movie end, and tested whether the gaze preferentially anticipated the impending action of the actor based on his FB. Since the FB movie was stilled after the light-up till the end, the monkey was never informed of the results or "correct responses" of the actor. Analysis windows consist of "central approach," "flash" and "post-flash" periods. In all movies, "flash" and "post-flash" periods were 1 s and 6 s, respectively. "Central approach" periods were 5 s in Movie 1, 4 s in Movie 2, and 1 s in Movie 3. The size of AOIs for false belief target AOI and non-target AOI were 78 × 120 (pixels) in Movie 1, 201 × 160 (pixels) in Movie 2, and 115 × 160 (pixels) in Movie 3 respectively relative to the screen resolution (1920 × 1080 pixels). The actions during the belief induction phase were inserted to control for several low-level cues—namely, that monkeys could not solve the task by simply expecting the actor to the first or last hidden box or the last box where the actor attended to (Figures S2C, S2I, and S2O). The order of the left-right location of the FB target was counterbalanced across scenarios within subjects. The left-right order for each scenario was counterbalanced as evenly as possible across individuals and the types (AS- and PS-) of the testing scheme. Though the target order in familiarization trials was fixed, the target location in the FB test was not predictable from the target order during familiarization. We analyzed whether the fixed order of presentation of the familiarization trials might have affected the animal's gaze behavior with repeated-measures ANOVA taking the effect of the location (left versus right) of the FB target into account.

Behavioral data analysis

We used two measures to evaluate the monkey's gaze bias toward the FB target: the first look direction and total looking time. The analysis time window was set from the time of the actor's re-appearance to the end of the movie, which lasted 8.00 to 11.46 s for respective movies. Rectangular areas of interests (AOIs) for the FB target and non-target were set to cover the boxes in Movies 1 and 2 (Figures 1E and 1J; Figures S2F and S2L) and hand-windows in Movie 3 (Figures 1O and S2R). We judge that the monkey's first look direction was to the FB target or non-target when the monkey's gaze entered the left or right AOI and stayed there for at least 100 ms for the first time during the analysis time window. We judge the trial to be "no look" if the gaze did not stay in either AOI for 100 ms during the test phase or if the gaze did not track the target movements during the belief induction phase. Specifically, if the animal did not look to the target quadrant less than 5% when the target was moved to the FB target box, then we classified the trials as 'no look'. We quantified the ratio of the total looking time for the target and non-target during the analysis time window using differential looking time score (DLTS) (Senju et al., 2009), which was defined as:

$$\mathrm{DLTS} = (\text{target looking time} - \text{non-target looking time})/(\text{target looking time} + \text{non-target looking time})$$

Statistics were performed using "R" (https://www.r-project.org). The statistical significance of the first look ratio and DLTS were evaluated with repeated-measures analysis of variance (ANOVA) with the fixed factor of first look directions (target or non-target) and the random factors of movie types and individuals. Additionally, ratio of the first looks to the target and non-target (Figure 2B), and mean number of first looks in the first trials for each movie (Figure S7A) in normal monkeys were also tested with Wilcoxon's signed rank test. In conducting Wilcoxon signed rank test, we replicated the procedures of a previous study (Krupenye et al., 2016), in which comparison of the paired data ("target-looking ratio" versus "non-target-looking ratios") were repeated with the number of animals (in the present study, N = 8). Data from different movie types were combined for each animal in this analysis. No-look trials were included as a part of the denominator in calculating the first look ratio, but not included in the analysis of the looking time.

We considered familiarization trials for Movies 1 and 2, excluding the very first trials when the animals were totally unfamiliar to the scenarios, as a true belief (TB) condition, and tested with Spearman's rank correlation test whether the animals developed TB attribution-like anticipatory gaze bias as the number of trials increased in terms of the first look score and DLTS.

We have conducted a permutation test to examine whether the first look bias (***the*** differential first look ratio between the target and non-target) and the DLTS were significantly different across conditions.

We have conducted binominal tests to examine whether correct first look ratio, the number of trials on which the participant made a correct first look divided by the number of trials on which the participant made a first look (correct or incorrect), are significantly higher than chance performance 0.5 in each four conditions.

Evaluation of low level abilities

To test whether inactivation of the mPFC affected perceptual, motor, or mnemonic abilities in hM4Di(+)CNO(+) and other conditions, we estimated the abilities of monkeys to track moving and hidden targets during the FB test movies by modified DLTS analyses. To quantify DLTS for the moving targets, the movement AOI as an area in which the agents were moving, and tested whether the percentage fixation time on the movement AOI versus anywhere else was more than would be expected by an even distribution. The analysis time window for moving target DLTS is indicated as yellow in the time indicating bars in Figure S4.

To quantify DLTS for the hidden targets, we defined the hidden target AOI on the wall behind which the actor was hidden while the monkey watched the puppet moving the object in Movie 3. To evaluate mnemonic ability excluding the effect of perception,

we quantified gaze bias to the hidden target AOI over a non-target AOI on the symmetric location by the DLTS. The time window for hidden target DLTS analysis is indicated as orange in the upper bars in Figure S4.

Viral vector preparation

The lentiviral vector for HiRet was prepared as described previously (Kato et al., 2011). The envelope plasmid contained FuG-B2 cDNA under control of the Cytomegalovirus enhancer/chicken b-actin promoter (pCAGGS-FuG-B2). The transfer plasmids contained the cDNA encoding hM4Di (Wakaizumi et al., 2016) downstream of the murine stem cell virus promoter. HEK293T cells were transfected with transfer, envelope, and packaging plasmids by the calcium phosphate precipitation method. Viral vector particles were pelleted by centrifugation at 6,000 x g for 16–18 h and resuspended in PBS. The particles were then applied to a Sepharose Q FF ion-exchange column (GE Healthcare) in PBS and eluted with a linear 0.0–1.5 M NaCl gradient. The fractions were monitored at an absorbance of 260/280 nanometer.

The peak fractions containing the particles were collected and concentrated by centrifugation through a Vivaspin filter (Sartorius, Goettingen, Germany). Proper concentrations of viral vectors encoding fluorescent protein were infected to HEK293T cells. To measure the genomic titer of the lentiviral vector, viral RNA in the vector stock solution was isolated with a NucleoSpinRNA virus kit (Clontech, NJ, USA), and the copy number of the RNA genome was determined by using a Lenti-X qRT-PCR titration kit (Clontech, NJ, USA).

Surgery

We microinjected lentiviral vectors incorporating hM4Di into the mPFC of five monkeys covering dorsomedial parts of Walker's area 8, 9, 10, 32 (Petrides and Pandya, 1994) under sterile conditions in a P2A operating room. Monkeys were initially sedated with medetomidine hydrochloride (0.1 mg/kg) and ketamine (5 mg/kg), intubated, and then anesthesia was maintained by inhalation of isoflurane (1.0%–2.0%) under mechanical ventilation. Surgery was conducted after confirming the disappearance of pain reflexes. During surgery, heart rate, oxygen saturation of peripheral artery, and end-tidal carbon dioxide concentration were continuously monitored, and ventilation was adjusted as needed. The monkey's head was fixed to a brain stereotaxic device (SN-3N, Narishige, Tokyo, Japan). After a midline skin incision, a rectangular craniotomy was made, ranging 31–51 mm anterior (A31–A51) to the external auditory canal and 10 mm on both left and right sides from the midline (L10–R10), with reference to the standard stereotactic coordinates of the macaque Atlas (Saleem and Logothetis, 2012). Under a microscope (OMK-2, Olympus, Tokyo, Japan), we made semicircular incision of the dura mater, and injected the hM4Di vector into a total of 8 sites in 3 monkeys (D, E, F). The stereotactic coordinates of the microinjection sites were (A44, L1), (A44, R1), (A42, L1), (A42, R1), (A40, L1), (A40, R1), (A38, L1), and (A38, R1). In one monkey (T), microinjection was done into 6 sites (A44, R1), (A42, R1), (A41, L1), (A39.5, R1), (A39, L1), (A36.8, R1). In another monkey (O), microinjection was limited to four sites in the left hemisphere. At each site, we injected the viral vector (2.0×10^{13} copies/ml) at two different depths. We injected 4 μL of the virus at a depth of 5 mm from the brain surface and 5 μL at a depth of 3 mm. Viruses were pressure-injected by 10 μL Hamilton syringe with a 30-gauge injection needle. The injection speed was set at 0.5 μl/min using a syringe pump (LEGATO nano, KD Scientific, MA, USA). After each injection, the needle remained *in situ* for 4–8 min to minimize backflow along the needle tract. After microinjection was completed, the dura, craniotomy, fascia and skin incision were closed layer by layer. Monkeys were given postsurgical analgesics (ketoprofen, 1 mg/kg/day, i.m.) and prophylactic antibiotics (ceftriaxone 40 mg/kg/day, i.m) for one week.

Drug administration

CNO (Toronto Research, Toronto, Canada) was dissolved in 50 μL of dimethyl sulfoxide (DMSO) (FUJIFILM Wako Pure Chemical Corporation, Osaka, Japan) in saline to a final volume of 2.5 ml. For behavioral testing, CNO was given at 3mg/kg intramuscularly, 60 min before the test movie presentation. The minimum interval between CNO injections was 48 h.

Electrophysiological recording *in vivo*

We conducted extracellular recordings from left hemisphere of Monkey F to assay DREADD-mediated neuronal suppression *in vivo*. An epoxy-coated tungsten microelectrode (FHC, Bowdoinham, ME, USA) was inserted into mPFC where the hM4Di vector was injected. The electrode was positioned and guided by a surgically implanted recording cylinder with a reference grid (Narishige, Tokyo, Japan), and was advanced to the target region from the dorsal surface of the cortex with a microdrive (MO903, Narishige, Tokyo, Japan). Signals were amplified by a factor of 5000, bandpass filtered between 0.3 and 250Hz, sampled at 1 kHz (nano2, SCOUT and trellis software, ripple, UT, USA). Visual stimulus presentation was controlled with the same apparatus for the behavioral tests. Monkeys' gaze was monitored during acquisition of the neurophysiological data as well as in other parts of our experiments. Visually evoked responses to 10 s movies depicting animate or inanimate objects displaying simple articulated motions wereanalyzed to evaluate the effect of CNO injection to the hM4Di DREADD-expressing circuit. These movies show simple motions of human/non-human agents like ''the ball is just bouncing.'' Nineteen movie stimuli were presented in a random order excluding a stimulus bias during CNO administration. Visually evoked responses were evaluated during the initial 500 ms from the onset the stimulus presentation. Signals restored offline were normalized using z-scoring by the distribution of pre-stimulus period of –200 to 0 ms after onset. Peak-to-peak amplitudes of event-related potentials and event-related spectral perturbation (ERSP) based on Morlet wavelet transform were calculated. The trial-wise difference between the maximum voltage between 50 ms and 130 ms after stimulus onset and the minimum

voltage between 130 ms and 250 ms was measured for computing the peak-to-peak amplitude. Total ERSP power between 70 and 350 ms after stimulus onset was used for computing the spectral power. The averaged peak-to-peak amplitude and the total power during the baseline period (20 minutes before CNO application) and 4 test periods (0 to 20, 20 to 40, 40 to 60, and 60 to 80 minutes) after CNO injection were statistically compared with ANOVA and Bonferroni post hoc pairwise comparison between the baseline and other four periods. Data were pooled from four sessions across 248, 251,199,184 and 135 trials in respective periods in the hM4Di(+) CNO(+) condition and 226, 220, 238, 231 and 219 trials, respectively, in the hM4Di(+)CNO(−) condition. For all analyses, we used in-house MATLAB (The MathWorks, MA, USA) codes with the open source MATLAB toolbox EEGLAB (https://sccn.ucsd.edu/eeglab/index.php).

Histology

We conducted histology with the minimum number of animals required to verify whether the hM4Di expression in the mPFC was as intended and reproducible. After completion of the behavioral experiments, two monkeys (O, E) were deeply anesthetized with sodium pentobarbital (75 mg/kg/day, i.m.) and perfused with 0.1 M phosphate-buffered saline (PBS) and 4% paraformaldehyde in 0.1 M PB. Brains were removed from the skull, then cryoprotected in 10, 20 and 30% sucrose and 0.02% Sodium Azide in 0.1 M PB at 4°C until they sank. The brain was sliced into coronal sections at a thickness of 50 μm as previously described (Hasegawa et al., 1998; Nakahara et al., 2016), and sorted into 2 series. One series of sections was stained for Nissl with 1% Cresyl violet (Cresyl violet acetate; Acros, Geel, Belgium) at 800 μm interval and coverslipped. Borders between each brain region as well as the white matter/gray matter border were determined by the nearest neighbor Nissl section according to the standard cytoarchitectonic criteria (Saleem and Logothetis, 2012; Walker, 1940). The other series of slices was blocked in blocking solution (0.3% H_2O_2 and 1% skim milk) for immunostaining of hM4Di and rabbit (1: 1000, Santa Cruz Biotechnology, sc-9109) or mouse (1:100, Chemicon international, MAB1576) anti-muscarinic acetylcholine receptor M4 antibody, with 2% normal donkey serum and 0.1% Triton X-100. After further washing, we incubated those slices with biotin-SP affinipure donkey anti-rabbit (1:1000, Jackson Immuno-research, 711-065-152, 715-065-150) or anti-mouse (1:100, Chemicon international, 715-065-150) IgG antibody with 1% normal donkey serum. The signal was amplified using the VECTASTAIN ABC system (1:200, PK-6100, Vector Laboratories). For immunohistochemistry detection, expression was visualized with a 3,3′- diaminobenzidine (DAB) reaction using 0.04% DAB and 0.04% NiCl2 in 0.05M tris-buffer. We added 50 μL of 0.003% H_2O_2 in DW every 2 min during the reaction, up to 150 μl. The sections were mounted onto gelatin-coated slides, air-dried, and coverslipped. Sections were examined with a light microscope (FSX100;Olympus, Tokyo, Japan and BZ-X800; Keyence, Osaka, Japan). The three-dimensional reconstruction of the sections was conducted by FreeD (http://free-d.versailles.inra.fr/html/freed.html).

QUANTIFICATION AND STATISTICAL ANALYSIS

Statistical analysis is described above in the sections Behavioral data analysis and Electrophysiological recording in vivo.

DATA AND CODE AVAILABILITY

The data and code that support the findings of this study are available from the corresponding authors upon request.